Semiconductor Photocatalysis. Part 22.[1] Visible-Light Induced Photoreduction of CO_2 with CdS Nanocrystallites — Importance of the Morphology and Surface Structures Controlled through Solvation by *N*,*N*-Dimethylformamide

Shozo Yanagida,* Masashi Kanemoto, Ken-ichi Ishihara, Yuji Wada, Takao Sakata,† and Hirotaro Mori†

Material and Life Science, Graduate School of Engineering, Osaka University, Suita, Osaka 565

†Research Center for Ultra-high Voltage Electron Microscopy, Osaka University, Suita, Osaka 565

(Received January 27, 1997)

Carbon dioxide (CO_2) is reduced to CO on hexagonal CdS nanocrystallites (mean diameter of 4 nm) prepared in *N*,*N*-dimethylformamide (DMF) under visible-light irradiation with a quantum yield of 0.098 at $\lambda = 405$ nm in the presence of TEA as an electron donor. Solvation of the surface of CdS nanocrystallites by DMF or a related amide molecules should control the crystalline growth and stabilize the favorable morphology with a size quantization-effect. The effect of Cd^{2+} or H_2S on CO production and the emission behavior, and the effect of electron donors suggest an important role of the surface structures of CdS–DMF for photo-induced electron transfer to CO_2. The scope and limitation of the photoreduction of CO_2 with semiconductor nanoparticles are discussed.

The photoreductive activation of CO_2 under mild conditions has recently attracted much interest in view of the chemical utilization of CO_2 recovered from waste gas of electric-power plants as a scenario to cope with the global greenhouse effect of the earth.[2,3] Semiconductor photocatalysis is one of the most active research fields in line with this theme.[4—8]

Some semiconductor systems were found to be highly active for the reduction of CO_2 under UV-light irradiation. For example, Inoue and his group recently reported that Cd-loaded ZnS gives the highest efficiency for the production of formate (32.5%) at $\lambda = 280$ nm in the presence of 2-propanol as a sacrificial electron donor.[4,9—14] They commonly consist of nanocrystallites and their loose aggregates on which the size-quantization effect is operative, and a photo-formed highly negative electron with a long lifetime in the conduction band should play an important role in the photocatalysis. Furthermore, the photocatalysis depends not only on the energetics of the photoformed electrons, but also on the surface structures, as revealed in our recent studies on the photocatalysis of ZnS nanocrystallites.[14]

We recently reported that CdS particles (CdS–DMF) prepared in *N*,*N*-dimethylformamide (DMF) consist of nanocrystallites stabilized by DMF molecules, themselves,[15] and that CdS–DMF photocatalyzes a very effective electron transfer from triethylamine (TEA) as an electron donor to CO_2 molecules, leading to selective CO production with a high quantum yield of ca. 10% under visible-light irradiation ($\lambda > 400$ nm).[10] These findings suggest that semiconductor nanoparticles with a sharp distribution in size should be easily prepared by using an organic solvent,[14] while preparation methods using stabilizing agents such as, surfactant vesicles,[16] polyphosphate,[17] thiols,[18] polymers,[19] colloidal silica,[11] porous glass,[20] zeolites,[21,22] or clays,[23] are noted. These stabilizing agents are unfavorable for elucidating the role of the surface structure in photocatalysis, because they affect the surface structures of nano-particles.

The success of the CO_2 photoreduction under visible-light irradiation is worth noting in view of the energetics of the CdS semiconductor, since the potential required for the transfer of a single electron to CO_2 is reported to be -2.21 V vs. SCE in DMF.[24] The flat-band potential of bulk CdS is reported to be -0.85 vs. SCE by Bard and -1.8 V vs. SCE by Meissner in acetonitrile.[25] Therefore raising up the conduction-band edge due to a size-quantization effect and the activation of CO_2 on the surface should be requisite for the effective photoreduction of CO_2 on CdS.

This paper reports on the scope and limitation of the visible-light induced photoreduction of CO_2 on CdS nanocrystallites prepared in organic solvents, while giving a discussion on the importance of the surface structures of CdS nanocrystallites for efficient photocatalysis, such as the DMF-solvated surface structure and surface sulfur vacancies as CO_2 adsorption sites.

Experimental

Materials. Cadmium perchlorate (guaranteed reagent (GR) grade) from Mitsuwa, cadmium acetate (GR grade), cadmium ni-

trate (GR grade), cadmium iodide (GR grade), and cadmium bromide (GR grade) all purchased from Wako Pure Chemical Industries were used as starting materials to prepare CdS nanocrystallites. Highly pure commercially available bulk CdS powders were purchased from Aldrich (CdS–Ald, 99.999%), Furuuchi (CdS–Furu, 99.999%), Mitsuwa (CdS–Mit, 99.999%), and Wako Pure Chemical Industries (CdS–Wako, 99.9%). Triethylamine (TEA, GR grade) was obtained from Wako Pure Chemical Industries and used after purifying by fractional distillation.

Preparation of CdS Nanocrystallites as Photocatalysts. CdS nanocrystallites (CdS–DMF) were prepared in a similar method to that reported by Ramsden et al., described as follows:[26] 5 ml of a DMF solution of $Cd(ClO_4)_2 \cdot 6H_2O$ (5 mM) was taken into a Pyrex tube. After purging with argon gas to remove dissolved oxygen, H_2S was introduced into the DMF solution under stirring on an ice bath, giving yellow color CdS nanocrystallites in DMF (CdS–DMF). CdS–DMF was used as a photocatalyst after again purging with argon gas to remove unreacted H_2S. CdS prepared similarly in acetonitrile and in methanol are denoted as CdS–AN and CdS–MeOH, respectively.

Analysis. H_2 and CO were analyzed by gas chromatography. Formate was analyzed by ion-exchange chromatography. Diethylamine, acetaldehyde, and ethanol were analyzed by GLC. The details concerning these analyses are described elsewhere.[14] Ketone, alcohol, and pinacol were analyzed by liquid chromatography using a Cosmosil–ODS column (4.6 mm × 150 mm) and a UV detector (at 230 nm) (Tosoh Model UV-8000). As an eluent, a mixture of methanol and buffered aqueous solution (KH_2PO_4–NaOH; pH = 7) (6 : 4 v/v mixture) was employed at an eluent rate of 0.5 ml min^{-1}.

Instruments for measurements of the UV-vis spectra, emission spectra, ^{13}C NMR, GC-MASS analysis of ^{13}CO are described elsewhere.[14]

General Procedure for the CdS–DMF–Catalyzed Photoreduction of CO_2. CO_2 was introduced into a stirred DMF solution (2 ml) containing CdS–DMF (CdS diatomic concentration = 2.5 mM, 1 M = 1 mol dm^{-3}), H_2O (crystal water contained in $Cd(ClO_4)_2 \cdot 6H_2O$ used as a starting compound for preparation of CdS–DMF resulted in the water concentration of 1.5 mM in the reaction solution) and TEA (1 M). The presence of TEA made the CdS–DMF solution slightly turbid when CO_2 was introduced. The resulting CO_2-saturated DMF solution was closed with a rubber stopper, and then irradiated under magnetically stirring with a 300-W tungsten halogen lamp through a saturated aqueous sodium nitrite solution filter ($\lambda > 400$ nm) in a water bath. The photoreaction with other CdS nanocrystallites (CdS–AN, CdS–MeOH, and CdS–H_2O) was carried out using the same solvent as that used for the preparation of the respective nanocrystallites. For reaction experiments with commercially available bulk CdS powder, DMF was used as a solvent.

Determination of Quantum Yield. The quantum yield for CO production was determined at $\lambda = 405$ nm under comparable conditions to those described above. Monochromatic light was obtained by using a Wacom xenon short-arc lamp (Model KXL-100F) and a Shimadzu Bausch monochromator. The intensity of incident light was monitored by tris(oxalato)ferrate(III) actinometry. The quantum yields were calculated by assuming that two photons are required for the formation of one molecule of CO.

High-Resolution Transmission Electron Micrographs. High-resolution transmission electron micrographs (TEM) were obtained with a Hitachi Model H-9000 TEM equipped with a tilting device (+− 10 degree) and operating at 300 kV (Cs = 0.9 mm). Images were recorded under axial illumination at an approximate Scherzer focus with a point resolution of better than 0.19 mm. The crystal structure was determined from the electron diffraction pattern. The particle-size distributions of CdS nanocrystallites were determined by measuring the sizes of 100 arbitrarily selected particles.

Results and Discussion

CdS-Catalyzed Photoreduction of Carbon Dioxide with Triethylamine in DMF under $\lambda > 400$-nm Irradiation. CdS nanocrystallites (CdS–DMF) prepared from $Cd(ClO_4)_2$ and H_2S in *N*,*N*-dimethylformamide (DMF) under cooling with ice and water showed excellent photocatalysis for CO_2 reduction in DMF under $\lambda > 400$ nm irradiation (Fig. 1).[10] After the induction period during the initial stage of irradiation, carbon monoxide (CO) was efficiently and selectively formed along with the evolution of a negligible amount of hydrogen (H_2). Diethylamine (DEA) and acetaldehyde were detected while maintaining the electron-balance with the CO formation during the initial stage of the reaction (Fig. 1). The leveling-off formation of acetaldehyde observed for the elongated reaction time is ascribed to the reactions: 1) acetaldehyde is converted to the amino alcohol in coupling with a radical formed in the oxidation and deprotonation of triethylamine[27] and 2) Claisen condensation of acetaldehyde occurs in such alkaline conditions. The selective formation of CO is in contrast with the predominant formation of formic acid observed for the photocatalytic reduction of CO_2 on ZnS nanocrystallites prepared in DMF.[14] The quantum yield for the formation of CO, measured after the induction period, was determined to be $\Phi_{1/2CO} = 0.098$ at $\lambda = 405$ nm. $^{13}CO_2$-incorporation experiments analyzed by mass spectroscopy and ^{13}C NMR showed the formation of ^{13}CO ($m/z = 29$), which confirmed that CO originates not from other organic substrates contained in the system, but

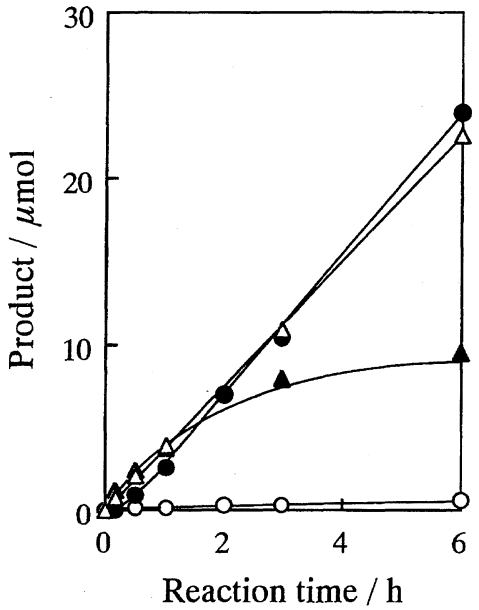

Fig. 1. CdS–DMF-catalyzed photoreduction of CO_2 in DMF with TEA under $\lambda > 400$-nm irradiation: (●) CO, (○) H_2, (△) diethylamine, and (▲) acetaldehyde.

from the CO_2 molecule. Neither H ^{13}COOH, (^{13}COOH)$_2$, H ^{13}CHO, nor $^{13}CH_3OH$ was detected.

When the photolysis with CdS–DMF was conducted in an argon atmosphere without CO_2, H_2 evolved as the sole reduction product about 10-times as much as that in the CO_2 atmosphere. The effect of added water was examined on the photocatalytic reduction of CO_2 with CdS–DMF. A CdS–DMF solution contained water (15 mM) derived from crystal water in $Cd(ClO_4)_2 \cdot 6H_2O$ used for preparing CdS–DMF. When the water content was further increased by adding water to the system (see Fig. 2), the CO production was gradually decreased to half. However, the formation of H_2 was not increased at all. These observations indicate that the reduction of CO_2 is predominant over that of water (or proton) in the present photosystem when CO_2 is present.

Photocatalysis on Various CdS Nanocrystallites. The photoreduction of CO_2 was examined by using other CdS nanocrystallites prepared in various solvents (Table 1). The photocatalytic activity of CdS nanocrystallites remarkably depended on the solvent used for the preparation. CdS–DMF gave the highest activity for CO evolution. CdS prepared in the solvents shown in the first group in Table 1, possessing an amide group as a common structure, showed a relatively high activity. On the other hand, CdS prepared in acetonitrile (AN) (CdS–AN) disclosed a lower activity. Furthermore, CdS prepared in methanol (CdS–MeOH) and in water (CdS–H_2O) showed almost no activity, demonstrating a contrast with the appreciable activity of ZnS–MeOH[14] and ZnS-0[9] for CO_2 photoreduction. Observations of the morphology of CdS nanocrystallites by TEM and their absorption spectroscopy showed that CdS particles prepared in DMF consist of nanocrystallites and showed a clear quantum size effect, as reported in a previous paper.[15] An EXAFS observation proved that the DMF molecules solvate to the surface cadmium atoms of the nanocrystallites by polarized oxygen atoms of the amide group.[15] Probably the solvation should control the growth and stabilization of CdS nanocrystallites. In the present paper we propose an important role of DMF molecules in the photocatalysis: the creation and stabilization of the CdS nanocrystallites as quantum boxes through effective solvation of the surface. The optimized activity observed for the CdS prepared in DMF could be attributed to a balanced solvation of the surface by DMF, in which CO_2 can replace DMF molecules solvating the surface in the reaction event.

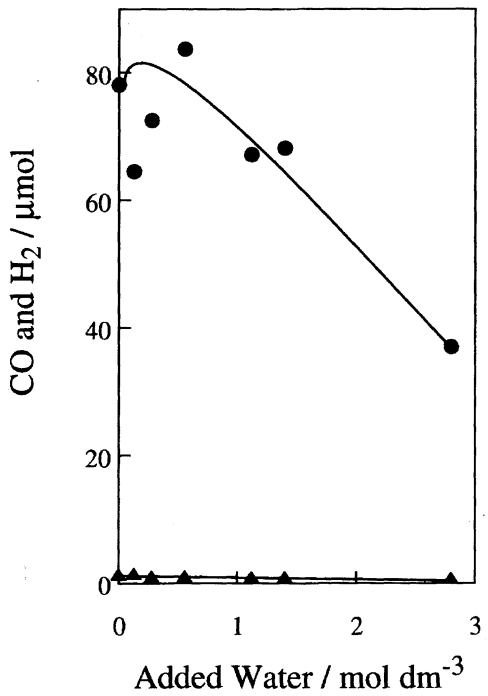

Fig. 2. Effect of added water on the CdS–DMF-catalyzed photoreduction of CO_2 with TEA under visible-light irradiation: (●) CO, (■) H_2.

Table 1. Photocatalytic Activity of CdS Nanocrystallites Prepared in Various Solvents

Solvent	Product/ μmol[a]	
	CO	H_2
$HCON(CH_3)_2$	83.7	1.1
$CH_3CON(CH_3)_2$	36.7	0.9
$HCON(C_2H_5)_2$	33.2	1.7
$HCONH_2$	29.8	1.8
N-Methyl-2-pyrrolidone	20.6	1.4
Tetramethylurea	19.8	0.7
MeCN	13.2	0.8
MeOH	1.3	3.1
THF	0	0
H_2O	0	0.3
CdS-Mitsuwa	0.2	0.8

a) Analyzed after irradiation ($\lambda > 400$ nm) for 10 h.

It is worth noting that the solution of CdS–AN was darkened during the photolysis experiments, which was ascribed to the formation of lattice Cd^0, as observed in the photocatalysis with CdS–MeOH in methanol.[28—30] The low efficiency of CdS–AN may be attributed to the formation of Cd^0 clusters on CdS–AN, suppressing the formation of the active sites for CO_2 adsorption.

A highly pure commercially available bulk CdS powder (CdS-Furu, CdS-Ald, CdS-Wako, and CdS-Mit) did not catalyze the photoreduction of CO_2. Inducing the quantum size effect of semiconductors is a requisite for the photocatalysis for CO_2 reduction.

The activity of CdS–DMF was influenced by cadmium salts employed as a source of Cd^{2+} for CdS, as was also observed in ZnS–DMF (Table 2).[14] Cadmium acetate gave the most active CdS–DMF. The resulting CdS–DMF was a yellow-colored transparent solution, and was found to be stable against the addition of TEA as an electron donor and photoirradiation, while other CdS–DMF became slightly turbid when TEA was added and the reaction system was irradiated. CdS–DMF prepared from cadmium perchlorate and nitrate also gave favorable activity for CO production. However, CdS–DMF prepared from cadmium bromide and iodide resulted in a very poor photocatalytic activity.

Table 2. Effect of the Counter Anion of the Starting Cd Salt on the Photocatalytic Activity

Cd salt	Product[a]/μmol	
	CO	H_2
$Cd(CH_3COO)_2$	120	1.7
$Cd(ClO_4)_2$	83.7	1.1
$Cd(NO_3)_2$	71.0	1.3
$CdBr_2$	4.0	0.7
CdI_2	4.2	0.4

a) Analyzed after irradiation ($\lambda > 400$ nm) for 10 h.

Recently, an EXAFS analysis of ZnS nanocrystallites prepared in DMF revealed that DMF molecules solvate to their surface, and that the solvation is affected by the coexisting anions derived from zinc salts employed for the preparation.[31] Therefore, the dramatic change in the photocatalytic activity of nanocrystallites may be explained as being due to the different surface solvation affected by coexisting anions.

TEM Observation of CdS Nanocrystallites. High-resolution transmission electron microscopy (TEM) has now revealed that freshly prepared transparent solutions of CdS–DMF and CdS–AN are composed of hexagonal nanocrystallites, as indicated by the lattice fringe in their TEM (Fig. 3). The turbid suspensions of CdS–MeOH and CdS–H_2O were found to be composed of cubic nanocrystallites. A TEM analysis also indicated that the particle size distribution of CdS–DMF and CdS–AN ranged from 3 to 5 nm in diameter, as shown in Fig. 4. Although the particle

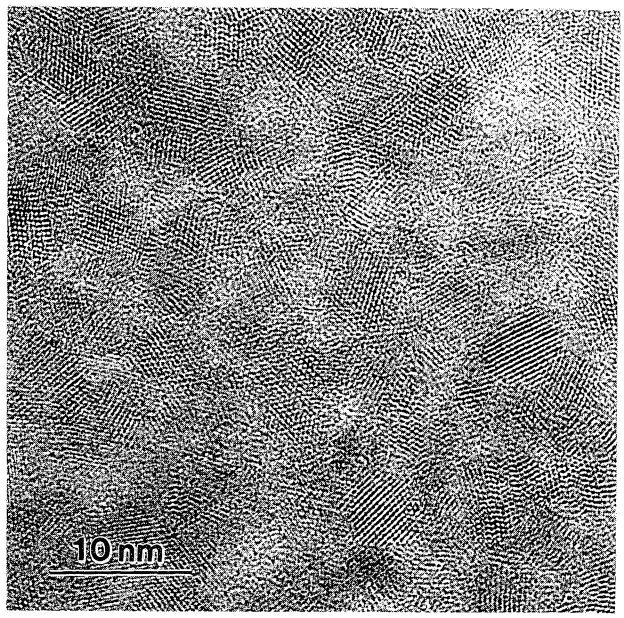

Fig. 3. Transmission electron micrograph of CdS–DMF.

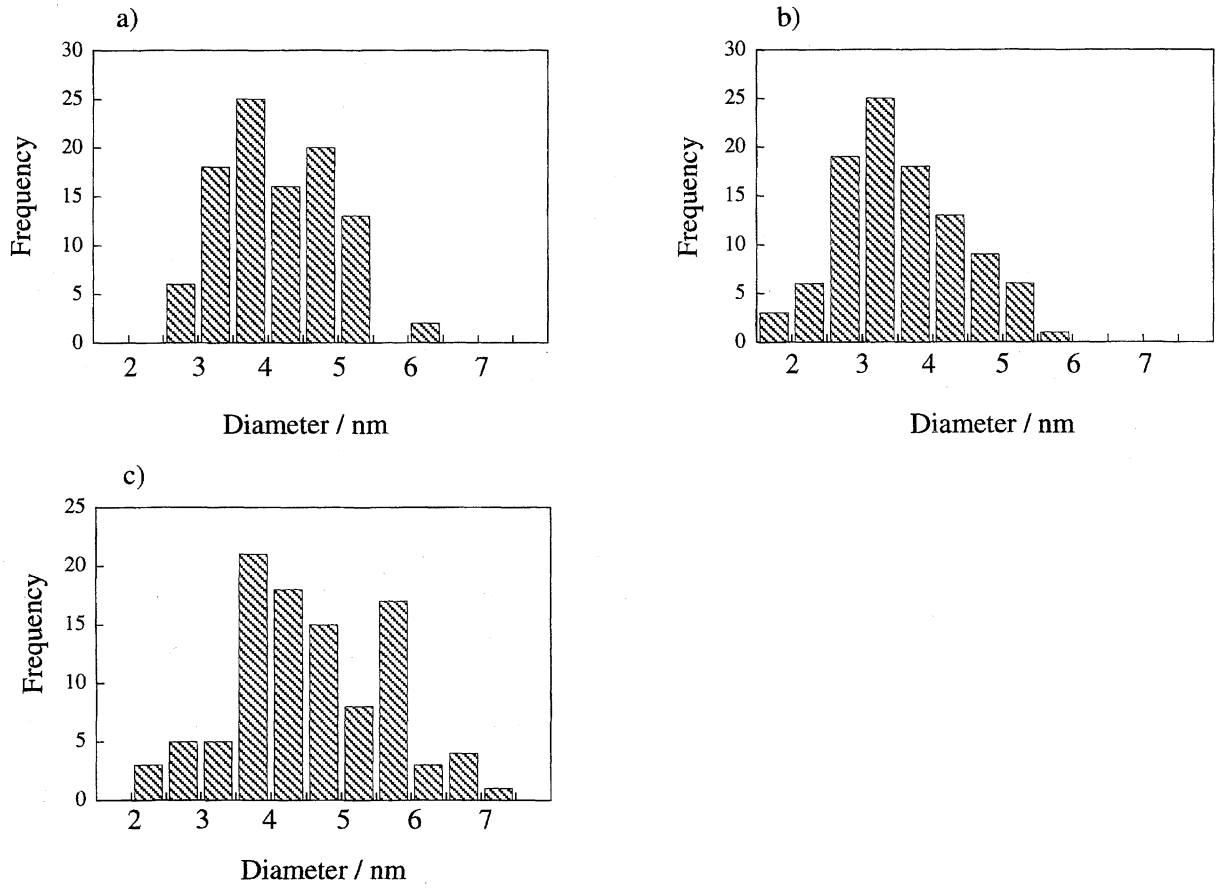

Fig. 4. Particle-size distribution of CdS determined by TEM: a) CdS–DMF, b) CdS–AN, c) CdS–H_2O.

size of CdS–H_2O observed in the TEM ranged from 2 to 7 nm, the colloidal solution of CdS–H_2O is considered to contain large aggregates of the particles, as reported for ZnS.[32] The large aggregates must have been out of sight of the TEM because of the large magnification. The determination of the particle size-distribution of CdS–MeOH was unsuccessful because the particles in CdS–MeOH gradually decomposed upon exposure to the electron beam during the measurement.

Absorption and Photoluminescence of CdS Nanocrystallites. The absorption spectra of CdS–DMF and CdS–AN were characterized by the steeper absorption threshold and the onset arising at the shorter wavelength than CdS–MeOH and CdS–H_2O (Fig. 5). These observations support that CdS–DMF and CdS–AN should consist of less aggregated nanocrystallites than the others. A red-shifted onset of CdS–MeOH and a further red-shifted onset of CdS–H_2O suggest that they should be aggregated, and that a protic solvent, such as MeOH and water, should assist in their aggregation. The rising up of the baseline observed for CdS–MeOH and CdS–H_2O at a longer wavelength ($\lambda > 500$ nm) was ascribed to scattering due to turbidity of their solutions.

The emission spectra of CdS–DMF were measured in DMF after a 2-fold dilution of the CdS–DMF solution with DMF. Figure 6 shows the emission spectra obtained by excitation at $\lambda = 400$ nm for CdS–DMF, as prepared, after 1-h aging in the dark, and after 1-h irradiation. The emission

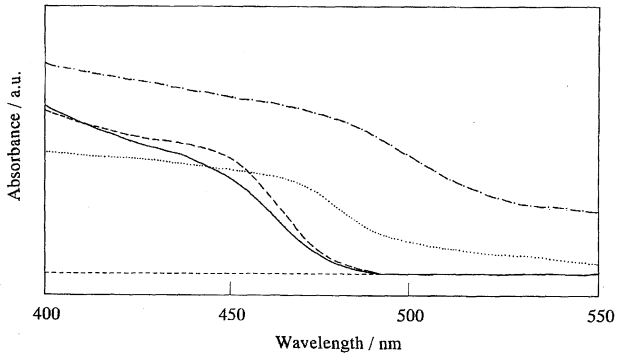

Fig. 5. Absorption spectra of CdS photocatalysts: (—) CdS–DMF, (- - -) CdS–AN, (····) CdS–MeOH, and (–·–) CdS–H_2O.

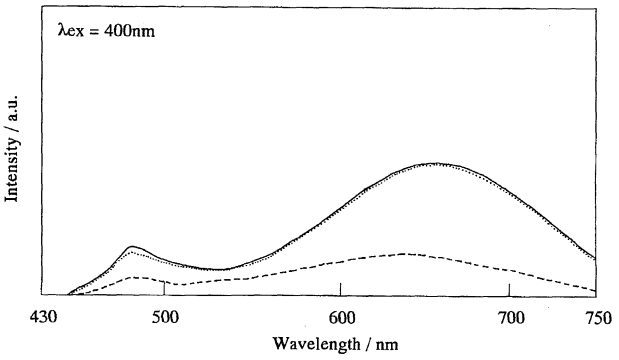

Fig. 6. Emission spectra of CdS–DMF obtained by $\lambda = 400$ nm excitation: (—) just after preparation, (- - -) aged for 1 h under dark, and (····) 1 h irradiation of aged CdS–DMF.

spectrum obtained for a fresh CdS–DMF solution consisted of bandgap emission ($\lambda_{max} = 480$ nm) and red emission from the surface states at a longer wavelength ($\lambda_{max} = 650$ nm). Both emissions have now been found to be changeable depending on standing in the dark and irradiation, as shown in Fig. 6. The intensity decreased upon standing in the dark, but was recovered by irradiation. Since the red-emission sites are assignable to sulfur vacancies, as reported,[33] these observations support the idea that such sulfur vacancies should exist or photoform on CdS–DMF. The emission was decreased when excess of H_2S was introduced into the solution, indicating that the surface sulfur vacancies should be occupied by the species of H_2S, HS^- or S^{2-}. On the contrary, the emission was increased upon adding Cd^{2+} into the system with a blue-shift in the maximum of the emission, indicating that the surface sulfur vacancies should be formed by surface reaction with the added Cd^{2+}.

Effect of the Cadmium Cation or H_2S on Photocatalysis. Figure 7 shows time-conversion plots of the photoproduction of CO in the presence of Cd^{2+} or H_2S added in excess. The induction period was gradually shortened with increasing the concentration of added Cd^{2+} (Fig. 7a). The addition of slightly excess Cd^{2+} increased the photocatalytic activity for the formation of CO. A similar enhancement in the CO production was also confirmed when excess Zn^{2+} was added to the ZnS–DMF system for CO_2 photoreduction.[14] The addition of a large excess (0.5 mM) of Cd^{2+}, however, caused a darkening of the CdS–DMF system, due to the photoreduction of excess Cd^{2+} to Cd^0 on CdS–DMF, resulting in a decrease of CO production.

On the other hand, when H_2S was added into the photosystem which was producing CO, the CO production was suppressed, but gradually recovered upon continued irradiation (Fig. 7b). The greater the quantity of added H_2S, the longer was the time required for the recovery. The observed induction period can be ascribed to the period required for photoformation of catalytically active sites on the surface. The active sites should be destroyed by the addition of H_2S and recovered by irradiation. The effects of excess Cd^{2+} or excess H_2S on the photocatalysis and the emission indicate that sulfur vacancies on CdS–DMF should be formed during visible-light irradiation, and serve as an active site for CO_2 photoreduction, as observed in the ZnS–DMF-catalyzed photoreduction of CO_2.[14]

Effect of Sacrificial Electron Donors. The potential of the valence band of CdS was estimated to be 0.7 V vs. SCE from the energy structure of single-crystalline CdS.[25] We examined the effect of some aliphatic amines as sacrificial electron donors on CO production, since they have oxidation potentials comparable with the valence-band potential of CdS (see Table 3).[34] TEA with E_{ox} (TEA/TEA$^{+\bullet}$) = 0.66 V vs. SCE in AN was found to be the best electron donor of the examined amines. The production of CO decreased in the order $Et_3N > Et_2NMe > Et_2NH$, which is in agreement with the properties indicating the ease of oxidation.

In general, aliphatic amines undergo one-electron oxidation giving intermediary radical cations (**1** in Scheme 1).

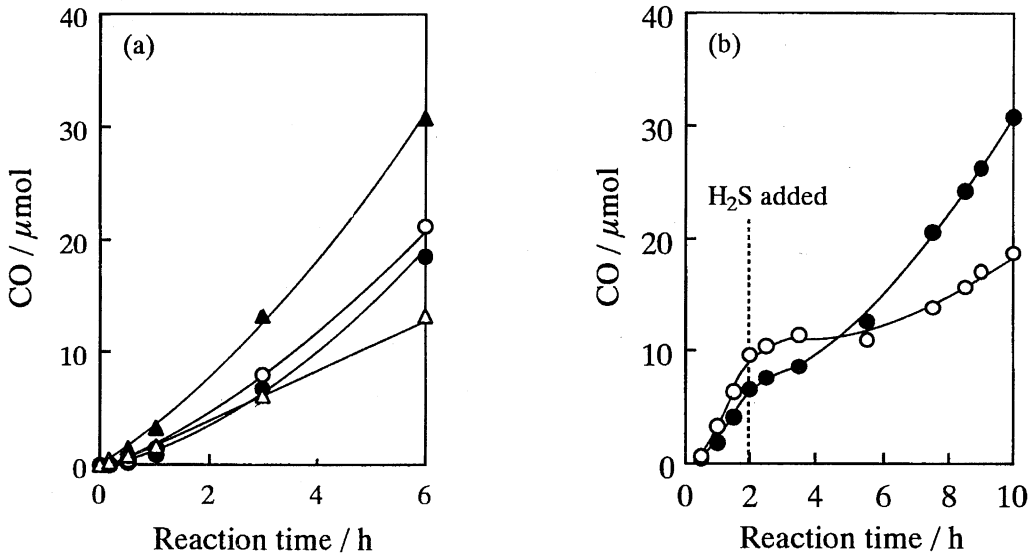

Fig. 7. Effect of the addition of an excess amount of Cd^{2+} (a) or H_2S (b) on the CdS–DMF-catalyzed photoreduction of CO_2: (a) Cd^{2+}; (●) no addition, (○) 0.025 mM, (▲) 0.25 mM, (△) 0.5 mM, (b) (●) 2 mmol, (○) 4 mmol.

Table 3. Dependence of the Photocatalytic Activity on the Electron Donors

Electron donor	CO[a]/μmol	E_{ox}[b]/V	1[c]/kcal mol^{-1}
Et_3N(TEA)	83.7	0.66	180.73
Et_2NMe	26.5	—	181.67
Et_2NH	5.7	1.01	186.02
(n-Pr)$_3$N	12.7	0.64	181.24
(n-Bu)$_3$N	7.1	0.62	180.33

a) The amount of CO formed during irradiation for 10 h. b) Oxidation potentials reported in the Ref. 17. c) Heat of formation of the radical cations calculated by MOPAC.

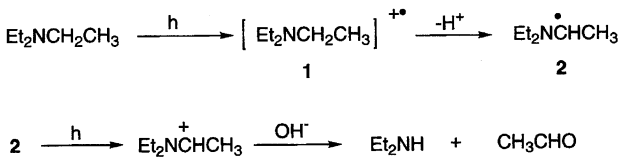

Scheme 1. Oxidation of TEA as an electron donor.

The heat of formation of the intermediary radical cations for the employed amines was calculated by semi-empirical molecular orbital calculations (Table 3). The heat of formation of the radical cations increased in the order $Et_3N > Et_2NMe > Et_2NH$, suggesting the ease of oxidation in the order $Et_3N > Et_2NMe > Et_2NH$, as is the order of their oxidation potentials. The dependence of the photocatalytic activity on the amines as an electron donor is explained as being due to the ease of oxidation by the hole photoformed in the valence band (Scheme 1).

Apparently, DEA, which has a potential more positive than TEA, $E_{ox}(DEA/DEA^{+\bullet}) = 1.01$ V vs. SCE in AN, could not be a good sacrificial electron donor. However, tri-n-propylamine and tri-n-butylamine produced only 13 and 7.0 μmol of CO under comparable conditions, as shown in Table 3, although they have more negative potentials than TEA: 0.64 and 0.62 vs. SCE in AN, respectively. These facts may suggest that the adsorption of electron-donating molecules on CdS–DMF could be of secondary importance for effective electron transfer on photoexcited CdS–DMF: the bulky alkyl groups in those amines hinder the adsorption.

Energy Structure of CdS–DMF. In order to estimate the reduction potential of the photoformed electron on CdS–DMF, the photoreduction of a series of ketones, whose reduction potentials range from −1.83 to −2.59 V vs. SCE, was attempted in DMF under the same conditions as CO_2 photoreduction (Table 4). Not only benzophenone (−1.83 V vs. SCE), but also 4,4′-dimethoxybenzophenone (−2.02 vs. SCE) and acetophenone (−2.14 V vs. SCE), were found to be photoreducible in the present photosystem, though neither acetone (−2.57 V vs. SCE) nor methylethyl ketone (−2.59 V vs. SCE) was reduced at all. It is also worth noting that the alcohols and pinacols were formed competitively in the CdS–DMF system, being in contrast with the selective formation of alcohols in the CdS–O–Cd system reported previously.[35] The mechanism should be quite in contrast with the sequential two-electron transfer mechanism through photoformed lattice Cd^0 on the cubic CdS–MeOH prepared in methanol, in which the electron transfer mediated by the lattice Cd^0 should proceed at a less-negative

Table 4. Photoreduction of Various Ketones by CdS–DMF

R–CO–R′		$-E^{1/2}_{red}$	Conv.[a]	Yield[a]/%	
R	R′	V	%	Alcohol	Pinacol
Ph	Ph	1.83[b]	100	20	44
p-MeOPh	p-MeOPh	2.02[b]	99	17	8
Me	Ph	2.14[b]	100	8	24
Me	Me	2.57[c]	0	0	0
Et	Me	2.59[c]	0	0	0

a) Irradiation for 6 h ($\lambda > 400$ nm). b) Polarographic half-wave reduction potentials in acetonitrile. c) Polarographic half-wave reduction potentials in 90% ethanol.

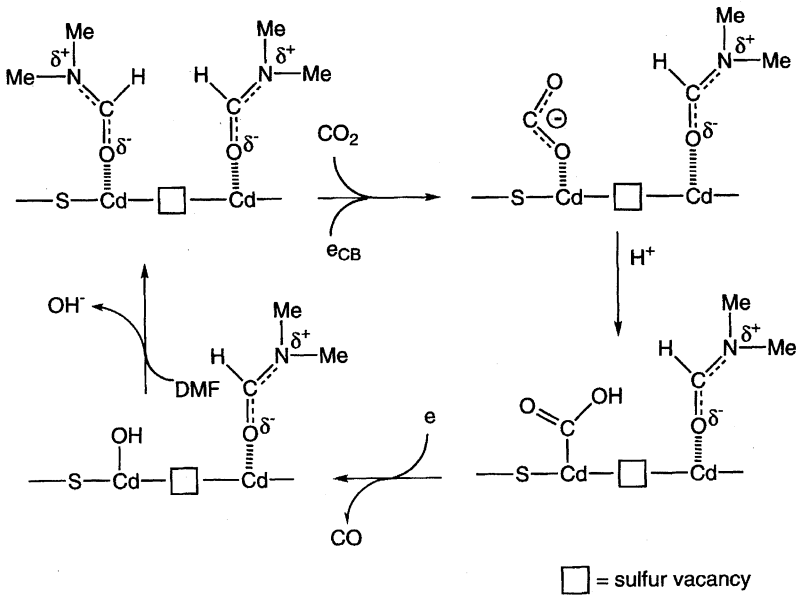

Scheme 2. Mechanism for photoresuction of CO_2.

reduction potential. These facts support the idea that the potential of the photoformed electron on CdS–DMF is negative enough to induce a one-electron reduction of CO_2 (−2.21 V vs. SCE in DMF).[24] In fact, our recent EPR measurements have revealed the formation of the CO_2 radical anion in the CdS–DMF-catalyzed photoreduction of CO_2 under visible-light irradiation.[1] This finding strongly supports the reduction of CO_2 through $CO_2^{-\bullet}$ on irradiated CdS nanocrystallites in the present system.

We previously reported that the cubic CdS nanocrystallites prepared from a methanolic solution of Na_2S and $Cd(ClO_4)_2$ have a reduction potential of around −2.00 V (vs. SCE) when irradiated with TEA as an electron donor.[35] On the other hand, highly pure commercially available bulk hexagonal CdS crystallites show a reduction potential of −1.90 V (vs. SCE) under comparable conditions.[28] The higher energy of the electron in the hexagonal CdS–DMF nanocrystallites can be ascribed to a more effective size-quantization effect than in the cubic ones.

Mechanism. As for the electrochemical reduction of CO_2 with a metal electrode in aprotic polar solvents, such as DMF, dimethyl sulfoxide, and propylene carbonate, it was reported that the reduction products are oxalate, CO, and a small amount of $HCOO^-$, and that the addition of a small amount of proton source (e.g., water) accelerates the formation of $HCOO^-$ and the further reduction of oxalate to glycolate.[24] In the present CdS–DMF photocatalysis, however, only the CO formation was observed and neither formate, oxalate, nor glycolate was produced, even in the presence of added water (< 4 mM). Furthermore, CO_2 was selectively reduced, and the photoreduction of protons to H_2 was suppressed in the presence of added water. The selective CO_2 reduction strongly suggests that the reductive electron transfer in the present system should proceed through effective adsorption of CO_2 molecules on CdS–DMF. Direct evidence supporting CO_2 adsorption was not obtained by FTIR or NMR, because the surface of CdS–DMF is stabilized through solvation by DMF molecules, as confirmed by EXAFS (in Scheme 2). This solvation through a cation-dipole interaction should create a cationic surface, preventing the adsorptive interaction of protons, resulting in a suppressed evolution of H_2. Neutral CO_2 could be adsorbed at active adsorptive sites and CO_2 adsorption might be competitive with appropriate solvation by DMF. The importance of the CO_2 adsorption was also disclosed concerning the photoelectrochemical reduction of CO_2 on a CdTe semiconductor photoelectrode.[36–38]

As active adsorptive sites, the surface lattice of Cd^{2+} in the vicinity of sulfur vacancies are conceived based on the following facts: (1) the addition of an appropriate quantity of Cd^{2+} shortened the induction period for CO production and enhanced the photocatalysis (Fig. 7a), (2) the addition of H_2S as a source of S^{2-} elongated the induction period, suppressing CO production (Fig. 7b), (3) the red emission (λ_{max} = 660 nm) due to the presence of sulfur vacancies[33] was diminished by the addition of excess S^{2-}.

From these points of view, we depict a plausible mechanism for the photocatalytic reduction of CO_2 on the photoexcited CdS–DMF nanocrystallites in Scheme 2.

The photogenerated conduction band electrons in DMF-solvated CdS–DMF nanocrystallites are once trapped by sulfur vacancies, giving (Cd^{2+} – e) pairs.[39] Electron donors quench photogenerated holes, leading to the formation of long-lived electrons with high reducing power as they are confined in the CdS–DMF quantum boxes.[40] CO_2 molecules on adsorptive sites readily undergo electron transfer, yielding a Cd^{2+} – carboxylic complex[41–44] by protonation. This complex should undergo successive electron transfer and reductive fission to give CO because the C–OH bond in the complex must be weakened by protonation, as proposed for metal–carboxylic complexes.[45–51]

Conclusions. The photoreduction of CO_2 to CO has been

achieved by using CdS–DMF nanocrystallites as photocatalysts and TEA as the most favorable electron donor, giving the highest quantum efficiency of 0.1 among the reported values for visible-light-driven CO_2 reduction with semiconductors. CdS–DMF in DMF has a structure of hexagonal nanocrystallites stabilized by appropriate solvation by DMF molecules, being regarded as self-organized quantum boxes. The confinement of highly energetic electrons in the quantum boxes, and effective adsorption of CO_2 molecules on the quantum boxes should contribute to the selective photochemical production of CO from CO_2.

This work was partly supported by a Grant-in-Aid for Scientific Research (A) from the Ministry of Education, Science, Sports and Culture (No. 06403023) and partly defrayed by the Grant-in-Aid on Priority-Area-Research on "Catalytic Chemistry of Unique Reaction Fields" from the Ministry of Education, Science, Sports and Culture (No. 07242248). This work was partly sponsored by New Energy and Industrial Technology Development Organization (NEDO)/Research Institute of Innovative Technology for the Earth (RITE).

References

1) H. Fujiwara, M. Kanemoto, H. Ankyu, K. Murakoshi, Y. Wada, and S. Yanagida, *J. Chem. Soc., Perkin Trans. 2*, in press.
2) J. Hansen, D. Johnson, A. Lacis, S. Lebedeff, P. Lee, D. Rind, and G. Russel, *Science*, **213**, 957 (1981).
3) "Proceeding of the International Symposium on Chemical Fixation of Carbon Dioxide," ed by K. Ito, The Chemical Society of Japan, The Research Group on Fixation of Carbon Dixoide, (1991).
4) T. Inoue, A. Fujishima, S. Konishi, and K. Honda, *Nature*, **277**, 637 (1979).
5) A. J. Bard, *Science*, **207**, 139 (1980).
6) M. A. Fox and M. T. Dulay, *Chem. Rev.*, **93**, 341 (1993).
7) A. Henglein, *Prog. Colloid Polym. Sci.*, **73**, 1 (1987).
8) A. Henglein, *Top. Curr. Chem.*, **143**, 113 (1988).
9) M. Kanemoto, T. Shiragami, C. Pac, and S. Yanagida, *J. Phys. Chem.*, **96**, 3521 (1992).
10) M. Kanemoto, K. Ishihara, Y. Wada, T. Sakata, H. Mori, and S. Yanagida, *Chem. Lett.*, **1992**, 835.
11) H. Inoue, T. Torimoto, T. Sakata, H. Moti, and H. Yoneyama, *Chem. Lett.*, **1990**, 1483.
12) H. Inoue, T. Matsuyama, B.-J. Liu, T. Sakata, H. Mori, and H. Yoneyama, *Chem. Lett.*, **1994**, 653.
13) H. Inoue, H. Morikawa, K. Maeda, and H. Yoneyama, *J. Photochem. Photobiol. A: Chem.*, **86**, 191 (1995).
14) M. Kanemoto, H. Hosokawa, Y. Wada, K. Murakoshi, S. Yanagida, T. Sakata, H. Mori, M. Ishikawa, and H. Kobayashi, *J. Chem. Soc., Faraday Trans.*, **92**, 2401 (1996).
15) H. Hosokawa, H. Fujiwara, K. Murakoshi, Y. Wada, S. Yanagida, and M. Satoh, *J. Phys. Chem.*, **100**, 6649 (1996).
16) J. H. Fendler, *Chem. Rev.*, **87**, 877 (1987).
17) H. Weller, *Angew. Chem., Int. Ed. Engl.*, **32**, 41 (1993).
18) Y. Nosaka, K. Yamaguchi, H. Miyama, and H. Hayashi, *Chem. Lett.*, **1988**, 605.
19) H. Uchida, S. Hirao, T. Torimoto, S. Kuwabata, T. Sakata, H. Mori, and H. Yoneyama, *Langmuir*, **11**, 3725 (1995).
20) J. Kuczynski and J. K. Thomas, *J. Phys. Chem.*, **89**, 2720 (1985).
21) N. Herron, Y. Wang, M. M. Eddy, G. D. Stucky, D. E. Cox. K. Moller, and T. Bein, *J. Am. Chem. Soc.*, **111**, 530 (1989).
22) K. Moller, M. M. Eddy, G. D. Stucky, N. Herron, and T. Bein, *J. Am. Chem. Soc.*, **111**, 2564 (1989).
23) H. Yoneyama, S. Haga, and S. Yamanaka, *J. Phys. Chem.*, **93**, 4833 (1989).
24) C. Amatore and J. M. Savéant, *J. Am. Chem. Soc.*, **103**, 5021 (1981).
25) D. Meissner, R. Memming, and B. Kastening, *J. Phys. Chem.*, **92**, 3476 (1988).
26) J. J. Ramsden, S. E. Webber, and M. Grätzel, *J. Phys. Chem.*, **89**, 2740 (1985).
27) S. Yanagida, H. Kawakami, Y. Midori, H. Kizumoto, C. Pac, and Y. Wada, *Bull. Chem. Soc. Jpn.*, **68**, 1811 (1995).
28) T. Shiragami, C. Pac, and S. Yanagida, *J. Chem. Soc., Chem. Commun.*, **1989**, 831.
29) T. Shiragami, S. Fukami, C. Pac, Y. Wada, and S. Yanagida, *Bull. Chem. Soc. Jpn.*, **66**, 2461 (1993).
30) T. Shiragami, S. Fukami, C. Pac, and S. Yanagida, *J. Chem. Soc., Faraday Trans.*, **89**, 1857 (1993).
31) H. Hosokawa, K. Murakoshi, Y. Wada, S. Yanagida, and M. Satoh, *Langmuir*, **12**, 3598 (1996).
32) S. Yanagida, M. Yoshiya, T. Shiragami, C. Pac, H. Mori, and H. Fujita, *J. Phys. Chem.*, **94**, 3104 (1990).
33) J. J. Ramsden and M. Grätzel, *J. Chem. Soc., Faraday Trans. 1*, **80**, 919 (1984).
34) L. A. Hull, W. P. Giordano, D. H. Ronsenblatt, G. T. Davis, C. K. Mann, and S. B. Mulliken, *J. Phys. Chem.*, **73**, 2142 (1969).
35) T. Shiragami, H. Ankyu, S. Fukami, C. Pac, S. Yanagida, H. Mori, and H. Fujita, *J. Chem. Soc., Faraday Trans.*, **88**, 1055 (1992).
36) I. Taniguchi, B. Aurian-Blajeni, and J. O. Bockris, *J. Electroanal. Chem.*, **157**, 179 (1983).
37) I. Taniguchi, B. Aurian-Blaheni, and J. O. Bockris, *J. Electroanal. Chem.*, **161**, 385 (1984).
38) J. O. Bockris and J. C. Wass, *J. Electroanal. Chem.*, **136**, 2521 (1989).
39) A. Henglein, *Ber. Bunsen-Ges. Phys. Chem.*, **86**, 301 (1982).
40) W. S. Pelouch, R. J. Ellingson, P. E. Powers, C. L. Tang, D. M. Szmyd, and A. Nozik, *J. Phys. Rev.*, **B45**, 1450 (1992).
41) D. A. Palmer and R. V. Eldik, *Chem. Rev.*, **83**, 651 (1983).
42) R. Ziesell, *Nouv. J. Chim.*, **7**, 613 (1983).
43) R. Ziesell, J. Hawecker, and J. M. Lehn, *Helv. Chim. Acta*, **69**, 1065 (1986).
44) J. L. Grant, K. Goswami, L. O. Spreer, J. W. Otvos, and M. Calvin, *J. Chem. Soc., Dalton Trans.*, **1987**, 2105.
45) T. Ogata, S. Yanagida, B. S. Brunschwig, and E. Fujita, *J. Am. Chem. Soc.*, 117, 6708 (1995).
46) S. Matsuoka, K. Yamamoto, T. Ogata, M. Kusaba, N. Nakashima, E. Fujita, and S. Yanagida, *J. Am. Chem. Soc.*, **115**, 601 (1993).
47) S. Sasaki, K. Kitaura, and K. Morokuma, *Inorg. Chem.*, **21**, 760 (1982).
48) S. Sasaki and A. Dedieu, *J. Organomet. Chem.*, **314**, C63 (1986).
49) S. Sasaki and A. Dedieu, *J. Organomet. Chem.*, **26**, 3728 (1987).
50) S. Sasaki, *J. Am. Chem. Soc.*, **112**, 7813 (1990).
51) S. Sasaki, *J. Am. Chem. Soc.*, **114**, 2055 (1992).